Raman spectroscopy of double-walled carbon nanotubes treated with H_2SO_4

E. B. Barros,[1,2,5] H. Son,[5] Ge. G. Samsonidze,[3,5] A. G. Souza Filho,[1] R. Saito,[2] Y. A. Kim,[4] H. Muramatsu,[4] T. Hayashi,[4] M. Endo,[4] J. Kong,[5] and M. S. Dresselhaus[5]

[1]*Departamento de Física, Universidade Federal do Ceará, Fortaleza, Ceará 60455-760, Brazil*

[2]*Department of Physics, Tohoku University and CREST, Sendai 980-8578, Japan*

[3]*Materials Sciences Division, Lawrence Berkeley National Laboratory, Berkeley, California 94720, USA*

[4]*Faculty of Engineering, Shinshu University, 4-17-1 Wakasato, Nagano-shi 380-8553, Japan*

[5]*Department of Electrical Engineering and Computer Science, Massachusetts Institute of Technology, Cambridge, Massachusetts 02139-4307, USA*

(Received 22 February 2007; revised manuscript received 1 May 2007; published 26 July 2007)

In this work, we performed a detailed study of the Raman spectra of double-wall carbon nanotube (DWNT) bucky paper samples. The effects of H_2SO_4 doping on the electronic and vibrational properties of the DWNTs are analyzed and compared to the corresponding effects on single-wall carbon nanotubes (SWNTs). Analysis of the radial breathing mode (RBM) Raman spectra indicates that the resonance condition for the outer wall nanotubes and the SWNTs are almost the same, indicating that the effect of the inner-outer wall interaction on the transition energies of the outer walls is weak compared to the width of the resonance window for the RBM peaks. The effect of H_2SO_4 on the RBM frequencies of the outer wall of the DWNTs is stronger for larger diameter nanotubes. In the case of the inner walls, only the metallic nanotubes were affected by the acid treatment, while the RBM peaks for the inner semiconducting nanotubes remained almost unchanged in both frequency and intensity. The G^+ band was seen to upshift in frequency with H_2SO_4 doping for both DWNTs and SWNTs. However, the effect of the acid treatment on the G^- band frequency for DWNTs was opposite to that of SWNTs in the 2.05–2.15 eV range, for which the acid treatment causes a ω_{G^-} upshift for SWNTs and a downshift for DWNTs. The G' band line shape of the DWNTs is explained in terms of four contributions from different components which are in resonance with the laser excitation. Two of these peaks are more related to the inner wall nanotube while the other two are more related to the outer wall.

DOI: 10.1103/PhysRevB.76.045425 PACS number(s): 73.22.−f, 78.30.Na

I. INTRODUCTION

Carbon nanotubes have been the subject of many studies over the past decade due to their unique mechanical and electronic properties which allow for an increasing number of applications. Most of the initial studies on carbon nanotubes were performed on multiwall carbon nanotubes (MWCNTs) and on single-wall carbon nanotubes (SWNTs). However, in more recent years, increasing attention is being given to double-wall carbon nanotubes (DWNTs) since they can be regarded as the simplest example of MWCNTs, and thus can be studied quantitatively and systematically. Also, DWNTs are promising for technological applications due to their robustness while retaining many of the highly desirable single-wall nanotube properties.

Recent calculations predicted that the interlayer interaction should have a stronger effect on the electronic structure of the inner wall, as compared to the effects on the outer wall.[1] It is also expected that the metallic character of one or both components of the DWNT can affect the inner-outer interlayer interaction. Such effects have not yet been clearly observed experimentally. Also, it is expected that the inner wall of the DWNTs will be somewhat protected by its outer wall from changes to the external environment, making them ideal samples for studying isolated, noninteracting tubes.

An important step towards the development of several technological applications of carbon nanotubes is to control their electronic properties. One possible way of controllably changing the carbon nanotube's electronic and vibrational properties is by transferring charges (electrons or holes) to the nanotube by means of intercalation and/or functionalization processes.[2–6] However, the process of doping the carbon nanotubes with the intercalant molecules and the effect of the intercalant on the nanotube properties are not yet well understood. The situation is complicated even further in the case of DWNTs, for which the doping process affects the inner and outer walls in very different ways, and where the metallic character of one (or both) of the walls plays an important role on the effect of doping on the DWNT electronic properties.[7] An increasing amount of work is now being dedicated to study the doping of carbon nanotubes with electrons and holes as a means to promote their possible technological applications. The study of both the intrinsic properties of carbon nanotubes and the interaction that occurs between the inner and outer walls in double-wall carbon nanotubes in their pristine and doped configurations is key to advancing the scientific understanding of the carbon nanotube properties and the development of suitable applications.

The recent development of a technique for obtaining high-purity double-wall nanotubes,[8,9] has opened new opportunities for research on the detailed interactions between the inner and outer tubes in DWNTs. We take advantage of this advance in the preparation of pure and H_2SO_4 treated DWNT bundle samples in the present work.

We report here a detailed study of the double-wall carbon nanotube Raman scattering properties and the effects of H_2SO_4 doping on their Raman spectra, which can, in most cases, be traced to the changes in the electronic and vibrational properties of the nanotubes. With this objective, Ra-

man scattering experiments were performed on a highly pure DWNT bucky paper sample using seven different laser excitation energies. To consider the effect of H_2SO_4 doping, part of the DWNT bucky paper was exposed to 99% sulfuric acid for 5 s. The short exposure time preserved the structural integrity of the sample but, nevertheless, produced significant changes in the experimental spectra to allow for a direct comparison between the pristine and acid treated samples. To better contrast the properties of the outer (large diameter) and inner (small diameter) nanotubes, a sample of highly pure SWNT bucky paper with a similar diameter distribution to that of the outer walls of the DWNTs studied here was also subjected to the same experimental conditions.

In Sec. II, the experimental setup used for obtaining the Raman spectra of the SWNT and DWNT samples is described. In Sec. III, the Raman spectra of pristine and acid treated DWNTs are analyzed and compared to the results for the SWNTs. This study is focused on the radial breathing mode (RBM), G band and G' band features. This paper is concluded in Sec. IV with a summary of the most important findings of the present work with comments about future research directions implied by the present work.

II. EXPERIMENT

Highly purified arc-derived SWNTs purchased from Iljin Company (Korea) were used without further purification and highly purified DWNTs were obtained by a chemical vapor deposition method and an optimized purification process, as previously described.[8,9] The two types of carbon nanotubes were each homogeneously dispersed in concentrated nitric acid for 5 h with the help of ultrasonication. It should be noted that both the SWNT and DWNT samples initially had large-sized bundles in the range of 20–50 nm. Thus, we were able to disperse both SWNT and DWNT samples only by strong nitric acid treatment. We also confirmed that there was no structural damage through this acid treatment based on scanning electron microscopy, tunneling electron microscopy, and Raman D band characterization.[8] Then, by filtering a stable suspension of SWNT and DWNT nanotubes [polytetrafluoroethylene (PTFE) filter, 1 μ], rinsing the resulting material with de-ionized water several times, drying it for 24 h in vacuum, and peeling off the paper from the PTFE filter, we obtained thin and flexible black-colored papers. Finally, these black-paper samples were dipped in concentrated sulfuric acid (97%) for a short time. No large changes in the D band spectra via chemical doping were observed, strongly suggesting that sulfuric acid treatment did not induce structural damage to the SWNT and DWNT samples.

The Raman spectroscopy experiments were performed in the backscattering geometry using a variety of laser excitation energies (E_{laser}) provided by an argon laser (2.41, 2.54, 2.71 eV), a krypton laser (1.916 eV), a Ti:sapphire laser (1.58 eV) pumped by the argon laser, a solid state laser (2.33 eV), and two dye lasers (with DCM and rhodamine 6 G as dyes) pumped with the argon laser. Four laser lines obtained using the dye laser were selected to be close enough to be within the resonance window for a given nanotube, allowing us to monitor the changes in the Raman spectra

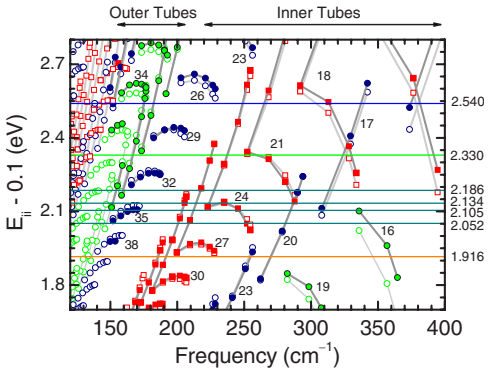

FIG. 1. (Color online) Kataura plot based on the ETB model (Ref. 11) in the region of transition energies and RBM frequencies for the SWNTs and DWNTs in our samples. The horizontal lines show the laser excitation energies (E_{laser}) used in the experiments. The numbers indicate the $2n+m$ families. The black and gray solid lines, respectively, refer to undoped and hole doped nanotubes (0.04 holes/carbon atom) (Ref. 7), as do the closed and open symbols, respectively.

which follow from the change in the resonance condition. The remaining laser lines were chosen to be approximately equally spaced from each other in energy, as well as covering the largest range of excitation energies available within our experimental setup. The light was focused on the sample using a 50× objective. The power irradiated in the sample was kept lower than 1 mW to avoid heating effects. Different acquisition times between 5 and 30 s were used for each sample in an attempt to optimize the signal-to-noise ratio of the Raman spectra. To avoid problems related to inhomogeneities in the sample, all spectra were taken on three to five different spots for each sample.

III. RESULTS AND DISCUSSION

Figure 1 shows the Kataura plot calculated for nanotubes within the range of the RBM frequencies expected for the nanotubes in the sample and with transition energies (E_{ii}) close to the excitation energies (E_{laser}) used in the experiment. In the figure, we show the range of RBM frequencies expected for the inner and outer walls of the DWNTs within the samples studied in this work. The diameter distribution for the SWNTs in these samples is closely the same as the distribution of diameters for the outer wall of the DWNTs studied in this work, and thus the spectra for DWNTs and SWNTs obtained here should show the same range of RBM frequencies. The Kataura plot shown in Fig. 1 was calculated using the extended tight-binding (ETB) approach, including many-body corrections by comparing the calculated results with those obtained experimentally on isolated SWNTs wrapped with SDS.[10,11] A downshift of 100 meV was applied to all transition energy values to account for the bundling effects.[12] In Fig. 1, ω_{RBM} is related to the tube diameter and chirality (d_t and θ, respectively) by $\omega_{RBM}=A/d_t+B+(C+D\cos 3\theta)/d_t^2$, with ω_{RBM} and d_t in units of cm^{-1} and nm, respectively.[10] The A, B, C, and D values used for constructing this plot were, respectively, 223 (228), 73 (14), −1.1

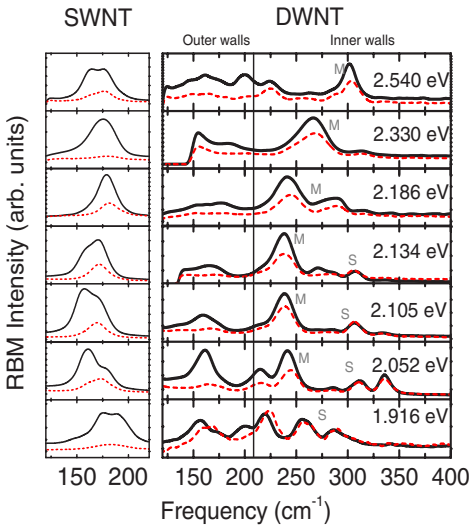

FIG. 2. (Color online) RBM spectra for DWNTS for 1.916, 2.052, 2.105, 2.134, 2.186, 2.330, and 2.540 eV excitation energies. Solid black (dashed red) lines are for undoped (H_2SO_4 doped) DWNT samples.

(−2.7), and −0.9 (−2.7) for semiconducting (metallic) nanotubes. This Kataura plot can be used as a guide for an evaluation of the resonance condition for each laser excitation energy and for guidance in interpreting the doping experiments. For this plot, the open symbols in Fig. 1 show the calculated transition energies when considering the effects of hole doping.[7]

A. Radial breathing mode spectra

The RBM Raman spectra for the pristine single-wall and double-wall nanotube samples are shown as black lines in Fig. 2. It should be noted that, in this figure, different intensity scales were used for SWNTs and DWNTs and for different laser energies. Therefore, the comparison of intensities in this figure is only valid within the same samples and laser excitation energies.

1. Inner-outer tube interaction effect on E_{ii} values

To gain insight into the electronic transition energies of the measured nanotubes, the experimental RBM peaks are assigned to the $2n+m$ families that give rise to most of the contributions to the RBM intensity, and in the case of the small diameter nanotubes, (n,m) assignments are tentatively made. The RBM frequencies and assignments are shown in Table I.

To understand the effect of the inner-outer tube interaction on the E_{ii} values of the outer wall nanotubes, we compare the RBM Raman spectra of the lower frequency RBM peaks (<200 cm^{-1}) for DWNTs and SWNTS with the Kataura plot. In the case of the SWNTs and the outer wall nanotubes of the DWNTs, agreement with the calculated Kataura plot could only be reached by considering that the E_{ii} values are further downshifted by 0.050–0.100 eV, indicating that the bundling effect in this system is somewhat stronger than previously observed.[12] Such is the case for the $E_{\text{laser}}=2.186$ eV spectra, where the peak at 178 cm^{-1} for SWNTs originates from nanotubes in the family $2n+m=32$. The intensity maximum of this RBM peak corresponds to the RBM frequency of nanotube (13,6), for which the calculated transition energy for SDS wrapped samples is approximately 2.255 eV, which indicates that the energy downshift resulting from the bundling effects on this particular tube is larger than what was observed previously by approximately 0.069 eV.[12] In the case of the DWNT samples studied with the same laser excitation energy ($E_{\text{laser}}=2.186$ eV), the Raman spectra show the contribution of many different peaks in the frequency region. Some of the observed peaks also originate from the nanotubes in family 32, as for the SWNT sample, indicating that the resonance condition in the two samples is similar. The same happens for other laser lines, where most of the RBM peaks observed for SWNT samples are also present in the DWNT RBM spectra. This result indicates that in DWNTs, the effect of the inner wall interaction on the electronic transitions of the outer wall nanotubes is weak compared to the resonance window of the RBM peaks for these tubes. It can be also noted that for DWNTs, the RBM spectra are much richer even in the region of the outer walls. There are two main factors contributing to this result. First of all, the diameter distribution for the outer walls in the DWNTs seems to be wider than that of the SWNTs, as is shown by the strong RBM spectral intensity below 160 cm^{-1} for $E_{\text{laser}}=2.186$ eV, which originates from nanotubes in families 34 and 37 or can be attributed to E_{44}^{S} transitions from larger diameter nanotubes. On the other hand, it is also understood that the interaction of the outer tubes with the inner wall can change the RBM frequency of the outer wall nanotubes, and this change will depend on the (n,m) structure of the inner wall carbon nanotube. Therefore, what shows up as a single peak for SWNTs should appear as a superposition of different peaks for DWNTs, corresponding to the same (n,m) outer wall nanotube interacting with different (n',m') inner wall nanotubes.[13,14] This effect is also related to the consistently larger full width at half maximum (FWHM) observed for the RBM peaks of the outer walls in the DWNT samples (see Table I).

It is now interesting to investigate how the inner-outer tube interaction changes the electronic transitions of the inner wall nanotubes and whether this effect is different for metallic and semiconducting inner walls. For this, it is useful to take a closer look at the RBM Raman spectra of the inner wall nanotubes obtained with the three laser excitation energies ranging from 2.052 and 2.134 eV, and to see how the Raman spectra evolve when the laser energy changes from the highest energy to the lowest one.

For $E_{\text{laser}}=2.134$ eV, the Raman spectra in the region of the RBM frequencies corresponding to the inner walls of DWNTs is composed of a strong broad band peaked at 237 cm^{-1} corresponding to metallic nanotubes from family 24, a weak feature peaked at 272 cm^{-1} corresponding to metallic nanotubes in family 21, and a broad band peaked at 284 cm^{-1} which can be related to nanotubes from family 20 (semiconducting). There are also two higher frequency peaks which appear at 308 and 335 cm^{-1}. However, out of these two, only the former has considerable intensity and corre-

TABLE I. Tentative assignment of ω_{RBM} for various laser excitation energies to $2n+m$ families and E_{ii} transitions for pristine DWNTs. The corresponding peaks for SWNTs are shown in square brackets when available. Large linewidth peaks are shown labeled with their maxima or by the frequency range within which they appear.

	DWNTs [SWNTs]				
E_{laser} (eV)	ω_{RBM} (cm^{-1})	FWHM (cm^{-1})	(n,m)	$2n+m$	
1.916	156 [151]	21 [13]		38	E_{33}^{S}
	[174,191]	[19, 19]		30	E_{11H}^{M}
	199,220	17,13		27	E_{11L}^{M}
	257	16	(11,1)	23	E_{22}^{S}
	288	20	(7,5)	19	E_{22}^{S}
2.052	160 [160,178]	20 [16,12]		35	E_{33}^{S}
	214	14		27	E_{11L}^{M}
	241	16		24	E_{11L}^{M}
	285	8		20	E_{22}^{S}
	309	11	(6,5)	17	E_{22}^{S}
	337	8	(6,4)	16	E_{22}^{S}
2.105	159 [155–171]	28 [13,15]		35	E_{33}^{S}
	215	20		27	E_{11L}^{M}
	238	19		24	E_{11L}^{M}
	308	12	(6,5)	17	E_{22}^{S}
	334	13	(6,4)	16	E_{22}^{S}
2.134	166 [159–172]	26 [12,13]		35	E_{33}^{S}
	237	21		24	E_{11L}^{M}
	272	7		21	E_{11L}^{M}
	284	12		20	E_{22}^{S}
	308	11	(6,5)	17	E_{22}^{S}
	335	11	(6,4)	16	E_{22}^{S}
2.186	153	23		34	E_{33}^{S}
	177 [178]	22		32	E_{33}^{S}
	241	25		24	E_{11L}^{M}
	286	21	(11,1)	20	E_{22}^{S}
2.330	$<$160 [170]	–[20]		37	E_{33}^{S}
	186 [180]	–[14]		29	E_{33}^{S}
	258	18	(8,5)	21	E_{22}^{S}
	270			21	E_{22}^{S}
	315	15		17	E_{22}^{S}
2.540	$<$160				E_{44}^{S}
	162 [160,177]	27 [17,19]		34	E_{33}^{S}
	200,224	[16,13]		26	E_{33}^{S}
	287	13	(6,6)	18	E_{11L}^{M}
	301	12	(7,4)	18	E_{11L}^{M}

sponds to the (6,5) nanotube which belongs to family 17. For $E_{\text{laser}}=2.105$ and 2.052 eV, the band at 237 cm^{-1} remains unaltered, while the small shoulder at a lower frequency, which shows up weakly for $E_{\text{laser}}=2.134$ eV, evolves toward a strong feature at 215 cm^{-1} for $E_{\text{laser}}=2.052$ eV arising from metallic nanotubes in family 27 in resonance with the lower energy E_{11L}^{M} transition. Also note that the contribution from the higher RBM frequency peaks increases as the laser excitation energy decreases to 2.052 eV. At this laser energy, a strong contribution is seen for two high frequency peaks at

approximately 309 and 336 cm^{-1}, which correspond, respectively, to the (6,5) and (6,4) nanotubes. It should be noted in Fig. 1 that the calculated transition energies for these two nanotubes (E_{22}^S) are 2.112 and 2.105 eV, and thus should be in better resonance with the 2.105 eV excitation energy. This fact indicates that the transition energy for these nanotubes is downshifted from the calculated energies by approximately 0.050 eV due to the inner-outer tube interaction. Since the calculated energies in Fig. 1 are downshifted by 100 meV compared to SDS wrapped SWNTs, the 0.150 eV downshift observed experimentally for these nanotubes characterizes the different interactions with the different wrapping materials (SDS and nanotube). On the other hand, the experimental results for the metallic nanotubes in families 24 and 27 are in good agreement with the calculated Kataura plot, indicating that, for these metallic nanotubes, the tube wrapping effect is ~50 meV weaker than that observed for the semiconducting nanotubes.

2. *Effect of* H_2SO_4 *treatment on the RBM spectra*

The effect of the H_2SO_4 treatment can be observed by comparing the intensities of the RBM Raman spectra for the pristine and H_2SO_4 treated samples (shown as a dashed line in Fig. 2). It can be noted that, for most laser excitation energies, the intensities of the RBM modes for the SWNTs and for the outer walls of the DWNTs are strongly suppressed by the interaction with H_2SO_4. It is interesting to point out that this suppression seems to be stronger for the lower frequency components of the RBM spectra, related to larger diameter nanotubes. This effect seems to be related to the fact that larger diameter nanotubes have a smaller band gap and thus are more easily affected by charge transfer. We can point out two possible effects that are usually believed to contribute to this strong intensity suppression: A damping of the nanotube RBM by the presence of a dopant molecule that prevents the radial movement of atoms and a change in the E_{ii} transition energies due to doping effects. In the first case, such vibrational damping should be accompanied by an increase in the RBM frequencies. However, except in the spectra for $E_{laser}=1.916$ eV, which will be discussed below, no evidence of a strong RBM upshift was observed after the acid treatment. A change in E_{ii} energy values seems more likely to be the cause of such an intensity suppression. However, it is striking that, for all of the excitation energies studied here, RBM intensities were all suppressed by the acid treatment and never showed an increase, which should be expected as E_{ii} values are changed into a better resonance condition. Therefore, although changes in the electronic transition energies are expected, there seems to be another process responsible for this suppression, which has not yet been elucidated. This decrease in intensity can originate from a broadening of the resonance window due to the interaction with the H_2SO_4 molecule. However, a more detailed study of the resonance window for doped isolated nanotubes is still needed in order to confirm or disprove this assumption.

In contrast, the higher frequency Raman peaks, corresponding to small diameter semiconducting nanotubes, remain almost unaffected by H_2SO_4 doping, in both frequency and intensity of the Raman peaks. The peaks in the intermediate frequency range (200–280 cm^{-1}) are affected by the acid treatment, but not as much as the larger diameter nanotubes. The reason for this discrepancy seems to be the metallic nature of these inner wall nanotubes. Recent work on Br_2 doped double-wall carbon nanotubes showed that the inner walls are more affected by charge transfer when they are metallic.[7] It should also be mentioned that H_2SO_4 doping caused a small frequency upshift in the peak that shows up at 238 cm^{-1} for the pristine sample. An RBM upshift is usually expected in the case of strong acceptor doping. However, since the same feature did not show a strong upshift with H_2SO_4 for the other laser lines, it is reasonable to assign this shift to a change in the resonance condition, enhancing the intensity of higher frequency peaks. This result is consistent with only a small amount of dopant being added to the system in our experiment. The dopant level was chosen to be small enough to allow the monitoring of these changes in E_{ii} and in the resonance condition.

This result can be used to make a better interpretation of the experiments. For instance, in the case of the 2.330 eV laser excitation energy, a weak feature is observed at 315 cm^{-1}, which can be tentatively assigned to either metallic nanotubes in family 18 or semiconducting nanotubes in family 17. However, the matching between the theoretical and experimental results is very poor, indicating that either the calculated RBM frequencies for such small nanotubes are upshifted related to the experimental results or the transition energies are quite different. To differentiate between these two interpretations, we observe that after the acid treatment, the band that is peaked at 270 cm^{-1}, and which can be identified with the metallic nanotubes in family 21, suffered a significant intensity suppression, while the intensity of the peak at 315 cm^{-1} remained almost unaltered. The difference in sensitivity to the acid treatment between the 270 and 315 cm^{-1} RBM peaks indicates that the latter peak originates from semiconducting nanotubes in family 17 and not from metallic tubes. That being the case, the RBM frequency calculated for this peak is higher than the experimental value by approximately 14 cm^{-1}.

3. *The RBM spectra for* $E_{laser}=1.916$ eV

The RBM spectrum for the DWNT samples obtained with $E_{laser}=1.916$ eV for the undoped sample shows five clear features peaked at 156, 199, 220, 257, and 288 cm^{-1}. The doping with H_2SO_4 does not suppress the lower frequency peaks as much as is observed for the remaining laser excitation energies or for the SWNT samples (see Fig. 2). For instance, the peak at 151 cm^{-1} for the pristine sample also shows up for the acid treated sample, with its frequency upshifted by about 7 cm^{-1} and showing a much larger linewidth. We argue that the high intensity and the frequency upshift observed for this peak originate mainly from the fact that nanotubes in family 38 are coming into a better resonance condition as a result of the doping. In this sense, the expected suppression of the RBM peaks is being balanced by a change in the transition energy which causes the nanotubes in family 38 to contribute more to the Raman spectra. It is also interesting to note that, while the acid treatment causes a strong intensity suppression for the peak at 200 cm^{-1}, the

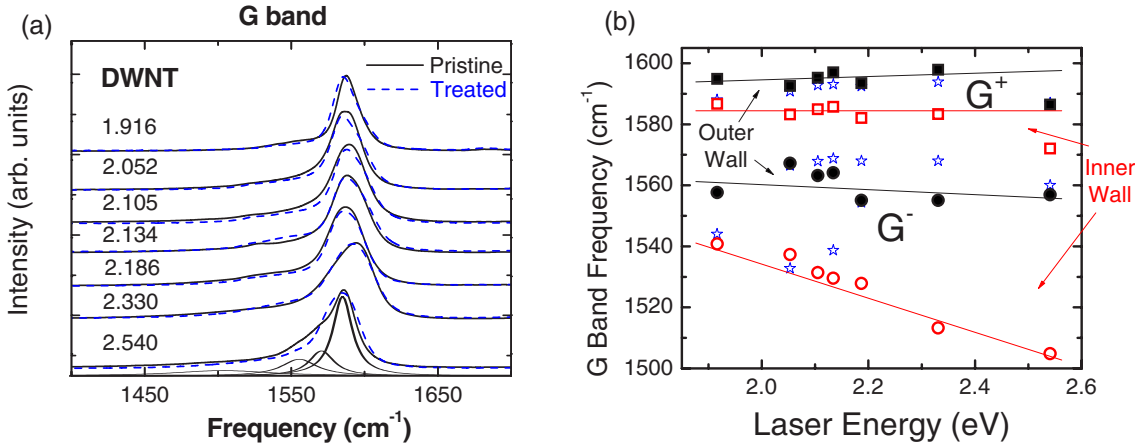

FIG. 3. (Color online) (a) *G* band spectral line shapes for pristine (solid lines) and H_2SO_4 treated DWNTs (dashed lines). The four best fit Lorentzians for the pristine sample are shown as thin dark lines for $E_{laser}=2.540$ eV. (b) Best fit frequencies for the *G* band peaks as a function of the excitation energy for the pristine DWNT samples. Squares and circles are for the G^+ and G^- bands in DWNTs, respectively. For comparison, the stars show the frequencies of these bands obtained for SWNTs. Solid and open symbols are for outer and inner tubes, respectively.

peak at 220 cm^{-1} did not show a large loss in intensity but instead showed a frequency upshift of ~ 5 cm^{-1}. These changes can be explained by considering that doping affects a metallic nanotube differently depending on its diameter and chirality. In this sense, those nanotubes in family 27, which are closer to the armchair chirality and also have a larger diameter, are being more affected by the acid treatment and thus are going out of resonance more strongly, while the tubes closer to zigzag chirality are less affected, thereby maintaining their resonance condition better. This result is in agreement with the fact that zigzag and chiral metallic nanotubes are, in fact, tiny band gap semiconductors, for which the magnitude of the gap decreases as the chiral angle of the nanotube approaches the armchair chirality, for which the band gap is zero.[15,16] The change in relative contributions from the different frequency peaks causes the observed frequency upshift.

It can be thus understood that the peak frequency upshifts observed for $E_{laser}=1.916$ eV are a consequence of a change of resonance conditions that results from the doping. This kind of effect can be more easily observed for $E_{laser}=1.916$ eV, due to the fact that this lower energy laser line tends to probe regions of larger diameter nanotubes, for which there is a large number of different nanotubes with similar transition energies.

B. *G* band spectra

In Fig. 3(a), we show the Raman spectra obtained from pristine (solid lines) and H_2SO_4 doped (dashed lines) double-wall nanotube samples. Following previous works,[8] the *G* band line shape for the DWNTs was fitted to four contributions, two corresponding to G^+ and G^- peaks of the outer wall nanotube and the other two corresponding to the G^+ and G^- peaks of the inner wall nanotube. It is important to note that, in spite of the large width of the *G* band due to the presence of double peak structures, the profile observed for this band is characteristic of semiconducting nanotubes, having a negligible contribution from metallic nanotubes. This is an interesting result since, at least for the 2.052 and 2.186 eV excitations, the RBM spectra indicated a strong contribution from metallic nanotubes in families 21 and 24. The weakness of the metallic-like G_M^- profile on the Raman spectra of these nanotubes indicates that the Fermi level of these nanotubes is shifted away from the *K* point (where the valence and conduction bands cross each other for undoped armchair nanotubes). This can happen if there is a charge transfer process between the inner and the outer tube, as predicted by Zólyomi *et al.*,[17] or it can be a result from the purification method applied to the double-wall nanotubes which involved exposure to nitric acid. However, it is important to stress that the *G* band Raman spectra obtained for the 2.33 and 2.54 eV excitation energies, in comparison to the lower E_{laser} values, have a somewhat stronger metallic-like feature which is associated with the inner metallic nanotubes being in resonance.

In the case of SWNT samples (not shown here),[18] the contribution to the G^- band from metallic nanotubes could be observed well for $E_{laser}<2.15$ eV. For this reason, the SWNT *G* band spectra obtained for these laser energies were fitted to three peaks, one corresponding to the G^+ band (highest frequency) and the other two corresponding to the G^- band originating from semiconducting nanotubes (intermediate frequency) and metallic nanotubes (lowest frequency). The best fit frequency values obtained for the pristine SWNTs are shown as stars in Fig. 3.

Comparing the *G* band Raman spectra for the H_2SO_4 treated double-wall nanotube samples [shown as dashed lines in Fig. 3(a)] to those of the undoped samples,[19] it can be seen that, for most of the spectra, the line shape of the *G* band remains qualitatively unaltered after the acid treatment. However, a more quantitative analysis shows that the intensity of the higher frequency component of the G^+ band increases with the acid treatment. This result can also be understood in terms of the effects of a charge transfer to the outer wall nanotubes, which are upshifted in frequency due

to the doping with H_2SO_4, as also occurs for graphite intercalation compounds.[20] The greatest changes in the G band line shape were observed for E_{laser}=2.54 eV, for which the G band evolved from a two component structure, with a single sharp peak to a structure showing a strong BWF-like tail indicative of a highly metallic character. This metallic character mainly comes from the inner wall nanotubes (see Table I).

Figure 3(b) shows the frequency of the G band peaks for pristine DWNTs as a function of laser excitation energy. The G band profile was fitted to four main contributions, such that two of them arise from the inner wall (one G^+ and one G^-) and two from the outer wall (one G^+ and one G^-). Previous works[21] have assigned the lower frequency G^+ and the lower frequency G^- peaks to the inner (small diameter) nanotubes, while the higher frequency G^+ and G^- peaks are associated with the outer wall. Both G^+ peaks show a small upshift in frequency with increasing laser excitation energy, although the frequency for the G^+ band for E_{laser}=2.540 eV shows up at a much lower frequency than expected. This can be related to a strong contribution from larger diameter nanotubes in family 34, for which the resonance occurs with the E_{44}^S electronic transition. By monitoring frequency shifts of the G^+ band for the outer walls more closely, it can be seen that for E_{laser} between 2.052 and 2.134 eV, the frequency of the G^+ band increases with increasing laser energy, and for the 2.186 eV laser excitation energy, the G^+ band frequency decreases. For comparison, the stars show the frequencies obtained for the SWNT samples. In the case of SWNTs, the spectra were fitted to three contributions, two different G^- bands, one for metallic and one for semiconducting nanotubes, and one peak for the G^+ band. It can be noted that the overall behavior of the G band frequencies for different E_{laser} are similar for SWNTs and for the outer wall of the double-wall nanotubes. However, the frequency of the G^+ band for the outer wall in DWNTs is upshifted relative to that of SWNTs. The magnitude of this upshift is different for each laser excitation energy and is thus dependent on which (n,m) nanotubes are in a good resonance condition.

It is interesting to comment on the difference between the G^- band frequency for the outer (higher frequency) and the inner (lower frequency) tubes in DWNTs. This frequency difference is observed to increase with increasing laser excitation energy. Considering that the frequency of the G^- band is proportional to $1/d_t^2$,[22,23] and that the separation between the inner and outer walls in DWNTs is fairly constant, the frequency difference between the G^- bands for inner and outer tubes should be proportional to $1/d_T^4$, where d_T is the diameter of the outer tube. As seen in the Kataura plot of Fig. 1, increasing the laser excitation energies seems to probe smaller diameter nanotubes more sensitively, which explains the increasing difference observed in the G^- band frequency for the inner and outer walls of DWNTs.

The frequency of the G^- peak for the outer walls shows a very weak overall downshift with increasing laser energy. Also, the frequency of the peaks associated with the G^- band for the outer walls also showed up at a lower frequency than that observed for the SWNTs. This effect is more pronounced for E_{laser}=2.186 and 2.330 eV and is very weak for E_{laser}=2.450 eV, whereas a comparison for E_{laser}=1.918 eV could not be made since, for SWNTs, the contribution from metallic nanotubes to the G band Raman spectra dominated the line shape, while for DWNTs, the contribution to the G band comes mostly from semiconducting nanotubes, and thus the comparison between the two peaks is not relevant.

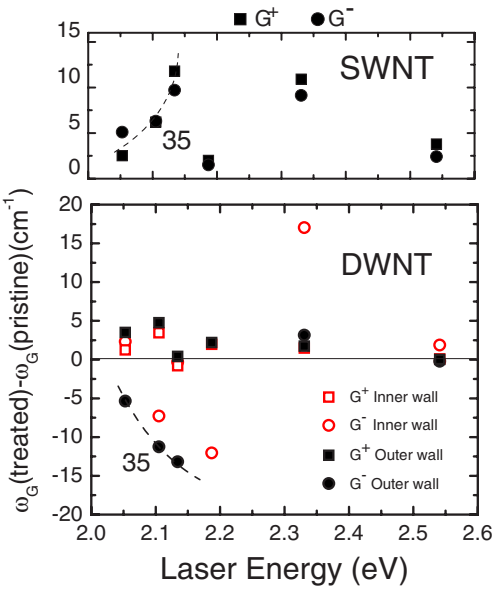

FIG. 4. (Color online) Frequency shift with H_2SO_4 doping of the G band components for (top) SWNTs and (bottom) DWNTs for different laser lines. The dashed lines in each figure are intended to highlight the behavior of nanotubes in family 35. Circles are for the G_S^- peak and squares are for the G_S^+ peak. For DWNTs, solid symbols are for the outer tubes while the open symbols are for the inner wall nanotubes.

Figure 4 shows the G band frequency shifts due to H_2SO_4 doping for SWNTs (top panel) and DWNTs (bottom panel). For the SWNTs, the acid treatment causes a frequency upshift in both ω_{G^+} and $\omega_{G_S^-}$. The magnitude of these shifts, $\Delta\omega_{G^+}$ and $\Delta\omega_{G_S^-}$, varied strongly with E_{laser}, showing a dependence on the specific nanotubes which are in resonance. However, all peaks were shifted toward higher frequencies for each laser excitation energy, and similar magnitudes were found for the G_S^+ and G_S^- frequency shifts for the same E_{laser}. For the DWNTs, the G^+ band showed a small upshift due to the acid treatment for most laser excitation energies. In agreement with previous experiments,[8] a stronger upshift was observed for the G^+ band associated with the outer walls than for the inner tubes. However, both peaks showed a small shift, indicating that although the outer wall protects the inner wall from environmental effects, it is still possible to measure some acid treatment effects from the inner wall nanotube vibrational properties. The much weaker frequency upshift observed after the acid treatment for the G^+ band in both the inner and outer wall nanotubes (0–5 cm^{-1}) as compared to SWNTs (2–12 cm^{-1}) may be indicative of a competition between the charge transfer effect on the inner and outer nanotubes and their interaction.

It is interesting to comment on the opposite shifts observed for the SWNTs and the outer wall of DWNTs for E_{laser}=2.052, 2.105, and 2.134 eV. It is noted from the RBM

spectra that these excitation energies span the different nanotubes in family 35, going from large chiral angle and large diameter nanotubes for $E_{laser}=2.052$ eV to small chiral angle and small diameter nanotubes for $E_{laser}=2.134$ eV. It can be noted that, in both cases, the effect of doping is always stronger for the smaller diameter nanotubes. However, the signal and magnitude of the shifts for the outer walls of the DWNTs and the SWNTs are opposite to each other. The exact process responsible for such effects has not yet been clarified. To better understand these processes, it is necessary to study the Raman spectra of isolated, single molecule, double-wall carbon nanotubes.

An interesting point that needs to be evaluated is the fact that, for $E_{laser}=2.052$, 2.105, and 2.134 eV, the RBM spectra show strong contributions from metallic nanotubes in family 24, while the *G* band for pristine nanotubes has a line shape which is characteristic of semiconducting nanotubes. It was proposed earlier that this effect can originate from an intrinsic charge transfer between the inner and outer nanotubes prior to the H_2SO_4 treatment, causing the Fermi level to be shifted away from the *K* point, and thus suppressing the BWF line shape of the metallic nanotubes in resonance. If this is the case, then the downshift observed for the G^- band originates from a change by the H_2SO_4 doping of the Fermi level back toward the *K* point. For $E_{laser}=2.330$ and 2.540 eV, the G^- band shows a weak BWF line shape, corresponding to the metallic nanotubes in resonance, indicating that the Fermi level of the metallic nanotubes in resonance with these laser excitation energies is close to, but below the crossing point (*K* point). This asymmetric peak is somewhat suppressed by the contribution from semiconducting nanotubes and the measured G^- frequency in Fig. 4(b) represents the mean value between the two contributions. In this case, hole doping by the H_2SO_4 molecule shifts the Fermi level away from the crossing point and weakens the observed BWF line shape, causing the mean G^- band frequency to upshift (as observed in Fig. 4). If this interpretation is correct, the charge transfer between the outer and inner nanotubes is larger in family 24 than in families 21 and 17.

C. G' band

The G' band spectrum for DWNTs can be decomposed into two, three, or four peaks depending on the excitation energy and on the nanotubes that are in resonance with the excitation laser. The presence of these different peaks was recently attributed to the interaction between the inner and outer tubes, in analogy to double layer graphene.[24] This interaction mixes the electronic bands of the two nanotubes, allowing four different double resonance Raman scattering conditions to occur. Following the case of double layer graphite,[24] the G' band profiles obtained for the four different excitation energies were fitted to four main contributions, while the small feature at ~ 2450 cm^{-1} is fitted to a single peak. Formally, this latter feature should also be composed of two to four peaks, for the different double resonance processes, but a single peak was used because the components cannot be resolved well in this experiment. The best fit parameters for the dispersion of these five peaks with respect to the excitation energy are shown in Table II, where ω_0 corresponds to the frequency at the *K* point. It can be seen that the slopes for the lowest and highest ($\omega_{G_1'}$ and $\omega_{G_4'}$) frequency peaks of the G' band are nearly the same (~ 75 cm^{-1}/eV), and thus $\omega_{G_4'}-\omega_{G_1'}$ is nearly constant (~ 66 cm^{-1}), almost the same value obtained for double layer graphene by Ferrari *et al.*, using 2.41 eV laser excitation.[24] As for $\omega_{G_2'}$ and $\omega_{G_3'}$, their slopes are also very close to one another (87 and 89 cm^{-1}/eV, respectively) and $\omega_{G_3'}-\omega_{G_2'}$ is also constant and equal to 28 cm^{-1}, nearly half of the frequency difference $\omega_{G_4'}-\omega_{G_1'}$ and about 40% larger than the separation between the corresponding peaks in double layer graphene (20 cm^{-1} for a 2.41 eV laser excitation energy).[24] The difference between $\partial\omega_{G_2'}/\partial E_{laser} \sim \partial\omega_{G_3'}/\partial E_{laser}$ and $\partial\omega_{G_1'}/\partial E_{laser} \sim \partial\omega_{G_4'}/\partial E_{laser}$ is small (~ 13 cm^{-1}/eV) compared to the linewidth of the G' band and can be attributed to experimental error.

TABLE II. Slopes for the linear fit to the frequency dependence of the G' band features in DWNTs. Here, ω_0 corresponds to the frequency at the *K* point.

Peak	ω_0 (cm^{-1})	$\partial\omega/\partial E_{laser}$ (cm^{-1}/eV)
0	2473	−15
1	2444	74
2	2434	89
3	2462	87
4	2510	76

A more detailed comparison between the frequency and dispersion observed for the G' band in SWNTs (indicated by stars in Fig. 5) shows very good agreement with peak 3 of the G' band in DWNTs. This follows from the fact that the mean frequency of the higher frequency peaks is in the same range as that of SWNTs, which have about the same diameter distribution as the outer walls of the DWNTs in this sample. Although this difference in frequency for the inner and outer tubes of the DWNTs has been previously observed experimentally,[7] it is not yet clear if this effect originates from a different double resonance condition for the inner walls compared to the outer walls, such as in the double layer graphene case, or if it is related to a softening of the phonon frequencies due to the very small diameter of the inner wall.

To help clarify this point, we extend the analysis to the peak denoted by 0 in Table II, at ~ 2450 cm^{-1} for SWNTs and DWNTs. In DWNTs, this peak has an overall lower frequency (by ~ 15 cm^{-1}) and a slightly weaker negative dispersion (-15 cm^{-1}/eV) when compared to SWNTs (-21 cm^{-1}/eV). Considering that in DWNTs this peak is a superposition of the contributions from the inner and outer walls, which cannot be separated well within the resolution of this experiment, this ~ 15 cm^{-1} downshift observed for the DWNTs indicates that the peak frequency for the inner wall nanotubes is downshifted by 15–30 cm^{-1} compared to that of the outer walls. Therefore, both the G' band (TO +TO) and the ~ 2450 cm^{-1} peak (TO+LA) have lower fre-

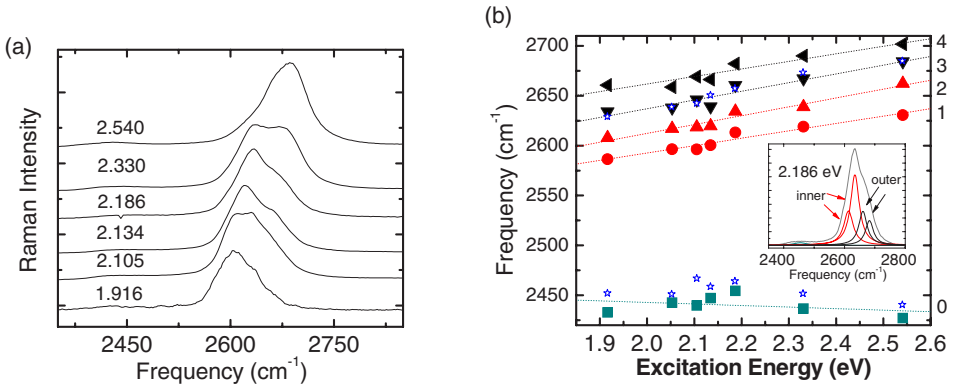

FIG. 5. (Color online) (a) G' band line shape for different laser excitation energies. (b) Frequencies for the different peaks composing the G' band and for the $\sim$2450 cm^{-1} peak corresponding to the LA+TO combination mode. The lines show a linear fit to the dependence with excitation energy. The stars (blue online) show the frequencies obtained for SWNTs. The inset shows the G' band line shape for E_{laser} =2.186 eV with the five Lorentzians used to fit it.

quencies for the inner wall tube (smaller diameter) than for the outer wall nanotubes (larger diameter). This result can be explained well as a softening of the TO phonon mode caused by the nanotube curvature.[25] On the other hand, a change in the resonance condition would lead to an opposite result. If in the case of inner wall nanotubes a different resonant condition were met which selected wave vectors closer to the K point (in the unrolled graphene sheet), this would, indeed, cause a downshift in the G' band frequency with respect to the outer wall nanotube, as observed in the experiment, but a frequency upshift would be expected for the LA phonon, which leads to an upshift of the $\sim$2450 cm^{-1} peak, contrary to the experimental results. Therefore it can be concluded that, opposite from the case of n-layer graphene where the resonance condition is the main factor determining the frequency of the G' band peaks, in DWNTs, the difference in phonon softening for the inner and outer walls plays a determining role for the G' band line shape.

The H_2SO_4 treatment has a strong effect on the G' band line shape. However, the frequencies of the four G' band features do not change by a significant amount through H_2SO_4 doping. Typically the $\omega_{G'}$ change is around 2–4 cm^{-1} (which is small compared to the linewidth of $\sim$40 cm^{-1} observed for the G' components), and the overall dispersion is increased by less than 10%. However, the main effect of the acid treatment is a change in the relative intensities of the peaks. To better analyze the relative intensities of the G' band peaks, we separate the spectra into only two contributions, one at lower frequency (G'_1 and G'_2), corresponding primarily to the inner wall nanotubes, and one at higher frequency (G'_3 and G'_4), corresponding primarily to the outer walls. In Fig. 6, the ratio of the integrated intensities of the lower to the higher frequency contributions ($I_{G'_1+G'_2}/I_{G'_3+G'_4}$) is shown for each of the laser excitation energies in the case of pristine (solid line and square symbols) and H_2SO_4 treated (dashed line and rhombus symbols) DWNT samples. It can be noted that this ratio tends to decrease with increasing laser energy toward a constant value. Pfeiffer *et al.*[26] attributed this behavior to the different scattering cross sections for the inner and outer nanotubes as a function of E_{laser}. In fact, the scattering cross section of the inner wall nanotubes was found to have a peak at approximately 2.3eV, decreasing very fast for higher laser excitation energies and slowly for lower excitation energies. In contrast, the ratio between the intensities for the inner and outer tubes in the present study does not decrease for the lower laser excitation energies.[26] This discrepancy can be related to the different diameter distributions of the samples studied here and those used in previous experiments.[26]

However, the decrease in the $I_{G'_1+G'_2}/I_{G'_3+G'_4}$ ratio with increasing laser excitation energy can be explained considering that for higher energy excitations, the E_{ii} values for small diameter inner nanotubes are very scattered, and thus not many different nanotubes will contribute for a specific E_{laser}. In contrast, the many different large diameter outer nanotubes will contribute to the G' band at approximately the same frequency, and thus decrease the $I_{G'_1+G'_2}/I_{G'_3+G'_4}$ ratio. This interpretation does not take into account the difference in the electron-phonon coupling for the inner nanotubes, which should be responsible for the large variation of the $I_{G'_1+G'_2}/I_{G'_3+G'_4}$ ratio for E_{laser} between 2.0 and 2.15 eV.

Comparing the intensity ratio between the lower and higher frequency contributions ($I_{G'_1+G'_2}/I_{G'_3+G'_4}$) for the pris-

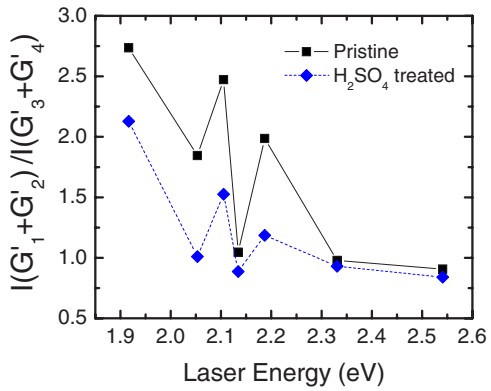

FIG. 6. (Color online) (a) Ratio between the lower (G'_1 and G'_2) and higher (G'_3 and G'_4) frequency contributions to the G' band line shape in DWNTs as a function of excitation laser energy. Squares are for pristine samples and rhombuses are for acid treated samples.

tine and the H_2SO_4 doped samples, it can be seen that the main effect of doping is to decrease the contribution from the lower frequency peaks to the G' spectra. The magnitude of this decrease varied from 7% to 45% of the original value for the undoped tubes.

IV. CONCLUSIONS

In summary, a detailed study of the Raman spectra of DWNTs was performed using seven different laser lines and the effects of H_2SO_4 doping on the electronic and vibrational properties were investigated. For comparison, the same set of laser lines was used to study SWNTs with a similar diameter distribution as that of the outer wall nanotubes in the DWNT sample studied here.

The analysis of the RBM spectra for SWNTs and DWNTs indicated that the electronic energy transitions for the SWNTs and the outer walls in the DWNTs are downshifted by 0.100–0.150 eV in comparison to the values obtained for SDS wrapped SWNT samples, indicating the magnitude of the change in the electronic transitions of the outer walls resulting from the inner-outer nanotube interaction. For the inner walls of DWNTs, the semiconducting nanotubes showed a downshift in the transition energies which was ~50 meV stronger than the metallic inner nanotubes. The H_2SO_4 treatment suppresses the RBM intensities for the SWNTs and for the outer walls of the DWNTs, and this effect is stronger for larger diameter nanotubes. In the case of the inner wall nanotubes, it is only the metallic nanotubes that showed a large decrease in RBM intensity after the acid treatment, while the intensity and line shape of the RBM feature for semiconducting inner wall tubes remained unaltered by H_2SO_4 addition.

The effect of H_2SO_4 doping on the G band spectra of DWNTs was opposite to that of SWNTs. In the latter, both the G^+ and G^- peaks showed an upshift after the acid treatment, while in the case of DWNTs, only the G^+ band showed an upshift (for which the outer tube is more affected), while for the spectra obtained with $E_{laser} < 2.15$ eV, the G^- band for the inner wall nanotubes showed a strong frequency downshift. This result was tentatively explained as an effect of metallic nanotubes contributing to the G^- spectra.

The G' band was fitted to four contributions, as in the case of double layer graphene. The frequency separation between the middle frequency G' peaks was found to be 40% higher that for the double layer graphene. The difference in frequency between the contributions from the inner and outer walls to the G' band is explained in terms of the softening of the phonon involved in the double resonance process due to the nanotube curvature. The H_2SO_4 doping was seen to decrease the relative contribution from the inner wall nanotubes to the G' band spectra.

ACKNOWLEDGMENTS

E.B.B acknowledges support from the Brazilian agency CAPES. R.S. acknowledges a Grant-in-Aid (Grant No. 16076201) from the Ministry of Education, Japan. E.B.B., H.S., G.G.S., J.K., and M.S.D. acknowledge support from NSF Grant No. DMR04-05538 and H.S. acknowledges the Intel Higher Education Program. Work is carried out using the Raman facility in the Spectroscopy Laboratory supported by the NSF-CHE 0111370 and NIH-RR02594 grants. A.G.S.F. acknowledges support from Brazilian agencies FUNCAP (Grant No. 985/03), CNPq (Grant Nos. 556549/2005-8, 475329/2006-6, and 307417/2004-2), Rede Nacional de Pesquisa em Nanotubos de Carbono, Rede Nacional de Nanobiotecnologia e Sistemas Nanoestruturados, Instituto do Milenio de Nanotecnologia, and Instituto do Milenio de Materiais Complexos (CNPq/MCT-Brazil).

[1] P. N. D'yachkov and D. V. Makaev, Phys. Rev. B **74**, 155442 (2006).
[2] A. M. Rao, P. C. Eklund, S. Bandow, A. Thess, and R. E. Smalley, Nature (London) **388**, 257 (1997).
[3] S. Bandow, G. Chen, G. U. Sumanasekera, R. Gupta, M. Yudasaka, S. Iijima, and P. C. Eklund, Phys. Rev. B **66**, 075416 (2002).
[4] P. Corio, A. P. Santos, P. S. Santos, M. L. A. Temperini, V. W. Brar, M. A. Pimenta, and M. S. Dresselhaus, Chem. Phys. Lett. **383**, 475 (2004).
[5] X. Liu, T. Pichler, M. Knupfer, J. Fink, and H. Kataura, Phys. Rev. B **70**, 205405 (2004).
[6] S. B. Fagan, A. G. Souza Filho, J. Mendes Filho, P. Corio, and M. S. Dresselhaus, Chem. Phys. Lett. **406**, 54 (2005).
[7] A. G. Souza Filho *et al.*, Phys. Rev. B **73**, 235413 (2006).
[8] Y. Kim, H. Muramatsu, T. Hayashi, M. Endo, M. Terrones, and M. Dresselhaus, Chem. Vap. Deposition **12**, 327 (2006).
[9] M. Endo, H. Muramatsu, T. Hayashi, Y. A. Kim, M. Terrones, and M. S. Dresselhaus, Nature (London) **433**, 476 (2005).
[10] A. Jorio *et al.*, Phys. Rev. B **71**, 075401 (2005).
[11] G. G. Samsonidze, R. Saito, N. Kobayashi, A. Grüneis, J. Jiang, A. Jorio, S. G. Chou, G. Dresselhaus, and M. S. Dresselhaus, Appl. Phys. Lett. **85**, 5703 (2004).
[12] C. Fantini, A. Jorio, M. Souza, M. S. Strano, M. S. Dresselhaus, and M. A. Pimenta, Phys. Rev. Lett. **93**, 147406 (2004).
[13] R. Pfeiffer, F. Simon, H. Kuzmany, and V. N. Popov, Phys. Rev. B **72**, 161404(R) (2005).
[14] H. Rauf, T. Pichler, R. Pfeiffer, F. Simon, H. Kuzmany, and V. N. Popov, Phys. Rev. B **74**, 235419 (2006).
[15] C. Zhou, J. Kong, and H. Dai, Phys. Rev. Lett. **84**, 5604 (2000).
[16] A. Kleiner and S. Eggert, Phys. Rev. B **63**, 073408 (2001).
[17] V. Zólyomi, A. Rusznyák, J. Kurti, A. Gali, F. Simon, H. Kuzmany, A. Szabados, and P. R. Surján, Phys. Status Solidi B **243**, 3476 (2006).
[18] E. B. Barros, Ph.D. thesis, Universidade Federal do Ceará, 2006.
[19] E. B. Barros *et al.* (unpublished).
[20] M. S. Dresselhaus and G. Dresselhaus, Adv. Phys. **51**, 1 (2002).
[21] Y. A. Kim, H. Muramatsu, M. Kojima, T. Hayashi, M. Endo,

M. Terrones, and M. S. Dresselhaus, Chem. Phys. Lett. **420**, 377 (2006).
[22] A. Jorio *et al.*, Phys. Rev. B **65**, 155412 (2002).
[23] O. Dubay and G. Kresse, Phys. Rev. B **67**, 035401 (2003).
[24] A. C. Ferrari *et al.*, Phys. Rev. Lett. **97**, 187401 (2006).
[25] A. G. Souza Filho *et al.* , Phys. Rev. B **67**, 035427 (2003).
[26] R. Pfeiffer, H. Kuzmany, F. Simon, S. N. Bokova, and E. Obraztsova, Phys. Rev. B **71**, 155409 (2005).